




A Robust Serial FBG Sensor Network with CDM Interrogation Allowing Overlapping Spectra

Marek Götten^{1,2}, Steffen Lochmann¹^a, Andreas Ahrens¹^b and César Benavente-Peces²^c

¹*Bereich Elektrotechnik und Informatik, Hochschule Wismar, Phillip-Müller-Straße 14, Wismar, Germany*

²*Escuela Técnica Superior de Ingeniería y Sistemas de Telecomunicación, Universidad Politécnica de Madrid, Crtra de Valenica, km 7, Madrid, Spain*


Keywords: Code-Division Multiplex, Fiber-Bragg-Gratings, Smart Structures, Serial Optical Sensor Networks, Optical Autocorrelation.


Abstract: Massive optical sensor networks gained a lot of attention in recent years. They offer new advances in the fields of smart structures and health monitoring. All serial optical sensor networks rely on multiplexing techniques that provide huge amounts of sensors in a single optical fiber. Wavelength-division multiplex (WDM) which has been established in many applications, is restricted to the spectral width of the used light source that needs to be shared by several non-overlapping fiber-Bragg-grating (FBG) spectra. Time-division multiplex (TDM) uses short impulses and relies on different sensor round trip delays to distinguish each single FBG. These short impulses and long round trip times lead to a low signal-to-noise ratio (SNR). Optical frequency-domain reflectometry (OFDR) offers a high spatial resolution of FBGs but only within a short fiber length. This contribution deals with a code-division multiplex (CDM) interrogation technique that provides numerous sensors in a single optical fiber, a better SNR, and a long range of distributed sensing points. It requires codes with good autocorrelation behavior which is characterized by certain criteria. The detectable criteria are limited which narrows significantly a search for best possible codes for the interrogation system. In this contribution, practical implementation limits such as the trigger timing and the achievable SNR are studied. Based on the introduced SNR definitions for CDM and WDM systems, a direct comparison is possible and it shows the superiority of the proposed CDM scheme. A network with 25 sensors operating at the same wavelength can provide a 2.67 dB improvement compared to WDM


1 INTRODUCTION

In the field of sensor technology, optical sensors, such as FBGs, gain a lot a attention. Their properties of being light, small, immune to electromagnetic interferences and capable of multiplexing, make them the preferred choice for many sensing applications (Rajan, 2015). Especially the multiplexing capability is in the focus of interest for applications like health monitoring (Glišić, 2016; Nawrot et al., 2017) and smart-structures, where optical fiber sensor networks can be integrated into materials (Braghin et al., 2013; Kim, 2004). Popular multiplexing techniques are WDM (Kersey et al., 1997), TDM (Wang et al., 2012) or optical frequency-domain reflectometry (OFDR) (Yamaguchi et al., 2015). This contri-

bution makes use of CDM that overcomes the restrictions of other multiplexing techniques. Unlike WDM, the optical sensors can spectrally overlap within the spectrum of the light source. Compared to TDM that makes use of a single short light impulse, a CDM interrogator collects several light impulses forming a code which significantly improves the SNR of the system. While OFDR works within short link networks (Yamaguchi et al., 2015), CDM has the potential of covering increased fiber lengths. The CDM technique requires codes with a good autocorrelation behavior (Abbenseth et al., 2016). The proposed interrogator for serial fiber optical sensor networks consisting of sensors operating at the same wavelength relies on the principle of CDM. In this contribution, the network can consist of several FBG sensors that partly reflect incident light according to their grating parameters, applied strain or temperature changes. In the following, the explanation of the interrogation

^a  <https://orcid.org/0000-0002-0938-2186>

^b  <https://orcid.org/0000-0002-7664-9450>

^c  <https://orcid.org/0000-0002-2734-890X>

principle is shown with the mentioned FBGs. Nevertheless, the principle is not limited to FBGs but rather works with every reflecting fiber optical sensor. CDM or code-division multiple access (CDMA) is already well known in the field of telecommunication, as the works by (Lee and Miller, 1998) or (Kitayama, 1998) indicate. Transferring this technique to sensor networks opens a new dimension of size considering spectral overlapping of sensors. In WDM systems, the spectral distribution of FBGs is limited to the spectral width of the light source and the operating range of each FBG that must not overlap with neighbouring FBGs during a measurement. (Abbenseth et al., 2016) shows that CDM in optical sensor networks allows spectral overlapping without losing track of the measured sensor. *Against this background the novelty of this contribution focuses on practical implementation limits such as the trigger timing and the achievable SNR. Based on the introduced SNR definitions for CDM and WDM systems a direct comparison is possible and it shows the superiority of the proposed CDM scheme.* The remaining part of the paper is structured as follows: Section 2 explains the CDM interrogation scheme. Section 3 discusses the different parameters influencing the overall performance. At the end, Section 4 concludes the work.

2 INTERROGATION PRINCIPLE

2.1 Interrogator Setup

Fig. 1 depicts the scheme of a CDM interrogator for serial fiber optical sensor networks. A light source provides the light that is launched into the sensor network and reflected by the FBGs. The spectral bandwidth should cover at least the operating region of each sensor in the network. The light source emits

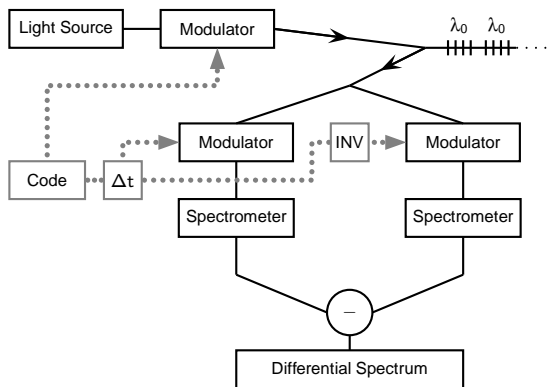


Figure 1: Scheme of CDM interrogation system.

continuous wave (CW) light that needs to be modulated for a CDM interrogation. The modulator is driven with code that is suitable for CDM; further details can be found in section 2.2. The modulated light is launched into the network with FBGs operating at the same wavelength λ_0 . The reflected light travels back and reaches the detector paths. It is split into two equal parts that are each modulated with a code again. This code is a time delayed version of the previous used code for the left path, the direct path, and for the right path, the inverted path, the code is time shifted and inverted. After the second modulation the light in each path is collected by a spectrometer, which performs the integration part of the correlation process. The inverted spectrum is subtracted from the direct spectrum which equals a differential spectrum that is used for peak detection. Further details about the setup are described by (Abbenseth et al., 2016) and (Götten et al., 2018).

2.2 CDM-interrogation Scheme

Having a deeper look into the maths of the interrogator, the scheme can be reduced to Figure 2. Light source (LS) and Modulator provide unipolar modulated light. The two detection paths contain each a modulator that works as a multiplication of the codes. Only, if a logical '1' reaches the modulator and it let's light pass (also a logical '1'), light reaches the sum, that represents the spectrometer collecting incoming light. Multiplication and summation equals mathematically a correlation; a unipolar - unipolar autocorrelation of the used code. Unipolar signal coding is the consequence of amplitude modulators applying simple on-off-keying of light. Introducing the inverted path, where the autocorrelation is performed with the inverted code, and calculating the difference, the result is a unipolar-bipolar autocorrelation which is explained in the work of (Götten et al., 2019) on the example of this interrogation setup.

Unipolar-bipolar correlations result in a scaled version of bipolar-bipolar correlations, as shown by (O'Farrell and Lochmann, 1994). The advantage is the ability of the autocorrelation function (ACF) to have low sidelobes. The products of the unipolar-

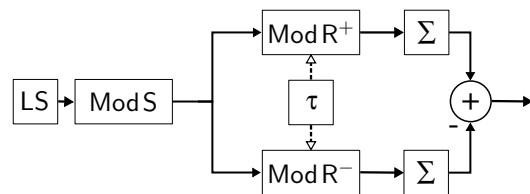


Figure 2: Principle of SIK.

unipolar correlation that are summed up can only be 0 or 1. The summed up products of bipolar-bipolar correlations can be -1 or 1. Therefore, the sum represented by each sidelobe can be close to zero if the mixture of -1 and 1 products is more or less equally distributed. In the unipolar-unipolar sum, the products can only add up, as no -1 product appears.

The ACF has the highest value in the autocorrelation peak for a time shift $\tau = 0$. Considering the value of the ACF as amount of light in the differential spectrum, the code reflected by an FBG that reaches the modulator exactly synchronous is the majority of light after calculating the difference. Assuming an ideal synchronization, in the direct path the whole light can pass the modulator and in the inverted path no light passes the modulator. Therefore, the difference between the sum of all light impulses of the code and no light results in a high value, mathematically the amount of chips of the code. Other reflected codes reach the detection path asynchronous to the modulators and therefore, not all light can pass or is blocked. Ideally, the amount of light passing each modulator is equal, so the difference results in zero. Depending on the code, the asynchronous reflected codes by other FBGs do not appear in the differential spectrum. This is achieved by a code that provides an ACF with very low sidelobes, ideally equal to zero, hence orthogonal or quasi-orthogonal codes.

2.3 Improvements of Interrogator Setup

The two detecting paths have to be identical to obtain a correct unipolar-bipolar correlation. Setting up the interrogator in a testbed requires identical equipment for both paths. To overcome this difficulty, the detection path is realized in a serial manner with only

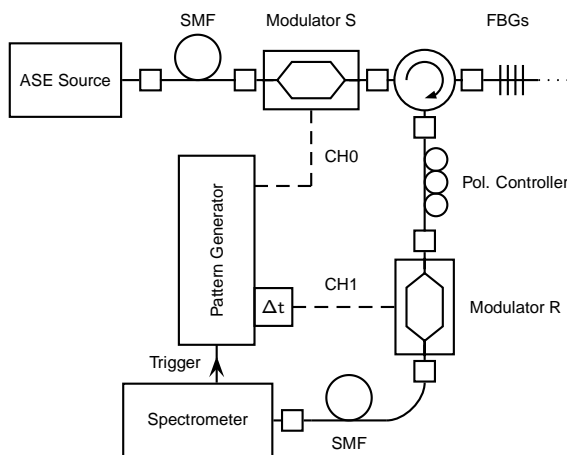


Figure 3: Scheme of a serial CDM interrogation system.

one modulator and one spectrometer. Direct and inverted path are now performed sequentially, where each measurement is repeated two times with direct and inverted code (Figure 3).

An amplified spontaneous emission (ASE) broadband light source provides the light that covers the full operating range of the FBGs in the network. The modulator S is driven with a code from a pattern generator. A circulator is responsible to guide direct light into the network and out of it into the detection path. The code is reflected by each FBG and has a different time delay introduced by different locations in the serial network. After the circulator, the light passes a polarization controller, the modulator R and reaches the spectrometer, which is a charge coupled device (CCD). The state of polarization (SOP) of the reflected light is unknown while the modulator is polarization dependent. Therefore, the polarization controller helps to improve the modulation result of the modulator. Modulator R is driven with the time shifted code. The time delay Δt matches the time light takes to travel from the modulator S via a distinct sensor to modulator R. Then the code is synchronized to that particular sensor. The pattern generator stores the direct and inverted code and is triggered by the spectrometer. The spectrometer emits a trigger signal when the integration time starts. Then the pattern generator emits through channel 0 the code and through channel 1 the time shifted code. The code is repeated so that the whole integration time is filled with the code. The time delay is introduced either by a channel time delay which is limited to 20 ns by the pattern generator settings or by rotating the code in the memory registers. Combining both methods, a coarse time shift is introduced by rotation of the code. Hence the shifting step equals the chip length. A fine time shift is added with the channel time delay of the pattern generator. The result is gapless adjustment of required time delays. The spectrum is stored on a computer and a second measurement with the inverted code is performed. Both spectra are subtracted from each other and the differential spectrum is used for peak detection. (Götten et al., 2019) provides more details about the correlation process with this interrogator.

3 INFLUENCES ON INTERROGATION SCHEME AND SETUP

The influences of a real testbed setup on the interrogation scheme have to be investigated. This section

presents two influences that affect the CDM results of the interrogator. As the interrogator needs to deal with different time delays, chip lengths and other temporal adjustments, the time delay of triggers and pattern generators has to be analyzed. Also the spectrometer, as one of the main parts of the correlation process is analyzed in more detail in comparison with a standard WDM system. A closer look at the modulators can be found in (Götten et al., 2019).

3.1 Trigger Scheme and Delays

Figure 4 shows the time behavior between integration time of the spectrometer and the code output of the second modulator. When the spectrometer starts to measure the spectrum, it emits a trigger that is connected to the data generator to start outputting the code. This delay time between trigger and the electrical code signal arriving at the first modulator is indicated by the blue part in the time diagram. This delay occurs for every single measurement of the spectrometer. After the delay, the first modulator starts with the code. This light travels through the network and is reflected at different locations by each FBG. Therefore, this code reaches the second modulator at different times, indicated by the light gray boxes in the diagram. The second modulation is synchronized to a specific reflected code and is time shifted to all other reflected codes. The time shift is depicted by the green part of the time diagram. The codes are repeated several times within one integration time. At the end, a part of the code is not covered by the integration time t_i , indicated by the hatched gray part of the time diagram.

During the trigger delay and the time shift, the second modulator is set to a logical '0'. The first modulator is set to logical '0' during the trigger delay as well. Then it starts modulating the light, according to the code. In the autocorrelation region, where both codes are multiplied by means of the second modulator, the error, introduced by an aperiodic autocorrelation is investigated in (Götten et al., 2018). Since a logical '0' does not prevent all light to pass the modulators, the spectrometer collects light at the beginning of the integration time. This light is attenuated by the offset of the first modulator, the reflectance of the FBGs and

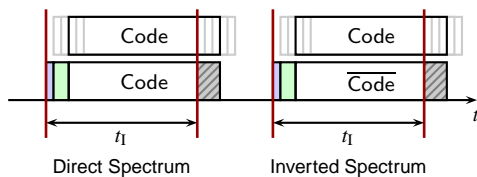


Figure 4: Temporal trigger scheme analysis.

the offset of the second modulator. Nevertheless, the collected light appears in the direct and in the inverted spectrum. The subtraction of both spectra cancels out this effect which shows the advantage of a sequence inverse keying (SIK) approach. The error introduced in the green region is depending on the code and the time shift or rather the synchronization point. Reflected codes can arrive before the second modulator starts to switch as well as after the second modulator starts to switch. For larger time shifts, the expected error increases, as well as the standard deviation of that error (Götten et al., 2018). For network lengths in the kilometer range, time shifts of more than 5 μ s can occur.

3.2 Spectral Influences of CDM Compared to WDM

In comparison with a WDM system, in the CDM processing all FBGs need to share the same wavelength. In the testbed, a CCD spectrometer is implemented that can collect only a certain amount of light that is represented in counts per wavelength range in the spectrum. In this testbed the spectrum is limited to 2^{16} counts that need to be shared by FBGs, as well as noise. The distribution inside a spectral peak for CDM is depicted in Figure 5. The two columns represent the amount of counts per spectrum, if all FBG are not strained, or heated so they all overlap. To achieve a cancellation of all interferences, the amount of light in both spectra (direct and inverted) needs to be equal, since the result is the difference out of these two. The light of the synchronized FBG (here FBG I-1) appears only in the direct spectrum, so nothing is subtracted from the desired signal. Therefore, the two parts of each FBG signal that distribute equally over

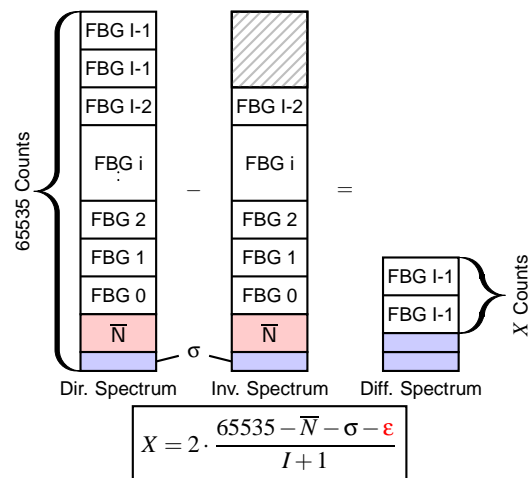


Figure 5: Spectral influences of a CDM approach with SIK.

Table 1: Parameters of testbed components.

Parameter	Value	Description
C	$2^{16} = 65535$	Maximum capacity of CCD spectrometer (BaySpec, FBGA)
I	25	Amount of serial sensors
\bar{N}	3000	Mean of noise of spectrometer (measured)
σ	30	Standard deviation of noise (measured)
ε	0	Summary of other influences (modulators, shape of light spectrum, ...)

both spectra for interference, is located only in the direct spectrum for the synchronized signal. Additionally, the noise of each measurement, divided into mean and standard deviation, is part of each spectrum and consumes a certain amount of light. The difference spectrum contains now only the two parts of the synchronized signal located in the direct spectrum and two times the standard deviation, since subtracting a random number from each other, the mean values cancel out and the standard deviation sum up. The theoretical available counts are calculated by the equation in the Figure using the example of 2^{16} counts. Since a WDM does not require a second measurement and a difference spectrum, the noise of the measurement cannot cancel out. Having a look at the SNR of the two different interrogation techniques, the advantage of a CDM approach can be shown.

The SNR in the CDM system can be calculated by

$$\text{SNR}_{\text{CDM}} = \frac{C - \bar{N} - \sigma - \varepsilon}{(I+1) \cdot 2 \cdot \sigma}. \quad (1)$$

C denotes the amount of counts provided in the spectrum, or rather the maximal possible height of a peak in the spectrum minus the noise values ($\bar{N} + \sigma$) and minus other influences ε . It is divided by the amount of sensors I plus 1, as depicted in Figure 5. It is also divided by two times the standard deviation σ that occurs as the only part of the noise in the differential spectrum. In comparison the SNR of a WDM system is derived by

$$\text{SNR}_{\text{WDM}} = \frac{C}{\bar{N} + \sigma}, \quad (2)$$

where the possible peak height C is divided by the complete noise consisting of mean value \bar{N} and standard deviation σ . The denominator of both SNRs influences its value. The larger the denominator, the worse the SNR. Using values from the testbed components in this contribution (see. Table 1), it shows the difference. For now, the other influences ε are set to zero.

$$\text{SNR}_{\text{CDM}} > \text{SNR}_{\text{WDM}} \quad (3)$$

$$\frac{2^{16} - 3000 - 30}{(25+1) \cdot 2 \cdot 30} > \frac{2^{16}}{3000+30} \quad (4)$$

$$40.07 \hat{=} 16.02 \text{ dB} > 21.63 \hat{=} 13.35 \text{ dB} \quad (5)$$

Due to the cancelling of the mean noise value \bar{N} in the differential spectrum, the SNR increases in comparison to a WDM system. To obtain the same SNR, as the WDM approach, other influences can increase up to

$$\begin{aligned} \varepsilon &\leq C - \bar{N} - \sigma - \text{SNR}_{\text{WDM}} \cdot (I+1) \cdot 2\sigma \quad (6) \\ &\leq 2^{16} - 3000 - 30 - 21.63 \cdot (25+1) \cdot 2 \cdot 30 \\ &\approx 28762 \text{ Counts.} \quad (7) \end{aligned}$$

Hence, these other influences on the spectrum of a CDM approach can be up to 43.88% of the maximum amount of counts, so the maximal possible peak height measurable by the implemented spectrometer. The SNR remains larger than in a WDM interrogator although the wavelengths are shared by all sensors in the network.

4 CONCLUSIONS

In this work, a CDM interrogation scheme for serial fiber optical sensor networks is introduced focusing on CDM-related issues and advantages. The trigger mechanism is temporally investigated. A delay introduced by the trigger has no influence on the resulting spectrum for peak detection. The spectral influences, due to wavelength overlapping, are analyzed and the advantage in terms of SNR are presented. The interrogation scheme is very robust against other possible imperfections. These imperfections such as the influence of the modulators as well as the spectrum of the source may accumulate up to 43.88% of the maximum measurable spectral power given by the spectrometer. Below this limit the CDM system performs superior to WDM in terms of the achievable SNR. Including previous works focusing on other aspects of a CDM approach, this CDM interrogation scheme is a promising step in a new dimension of massive sensor multiplexing in serial fiber optical sensor networks.

ACKNOWLEDGEMENTS

This work has been funded by the German Ministry of Education and Research (No. 13FH030PX8).

REFERENCES

- Abbenseth, S., Lochmann, S., Ahrens, A., and Rehm, B. (2016). Serial FBG sensor network allowing overlapping spectra. In Lewis, E., editor, *Sixth European Workshop on Optical Fibre Sensors*. SPIE.
- Braghin, F., Cazzulani, G., Cinquemani, S., and Resta, F. (2013). Potential of FBG Sensors for Vibration Control in Smart Structures. In *2013 IEEE International Conference on Mechatronics (ICM)*. IEEE.
- Glišić, B. (2016). Performance and Health Monitoring of civil structures and infrastructure using long-gauge and distributed Fiber Optic Sensors. In *2016 18th International Conference on Transparent Optical Networks (ICTON)*. IEEE.
- Götten, M., Lochmann, S., and Ahrens, A. (2018). Analysis of Non-Ideal Optical Correlation for Interrogating Overlapping FBG Spectra. In *2018 Advances in Wireless and Optical Communications (RTUWO)*, pages 154–160. IEEE.
- Götten, M., Lochmann, S., Ahrens, A., and Benavente-Peces, C. (2019). Detection Limits of Optical Auto-correlations with a CDM Interrogator for Overlapping FBG Spectra. In *2019 International Interdisciplinary PhD Workshop (IIPhDW)*, pages 106–109. IEEE.
- Kersey, A. D., Davis, M. A., Patrick, H. J., LeBlanc, M., Koo, K. P., Askins, C. G., Putnam, M. A., and Friebele, E. J. (1997). Fiber grating sensors. *Journal of Lightwave Technology*, 15(8):1442–1463.
- Kim, K. S. (2004). Dynamic Strain Measurement with Fiber Bragg Grating Sensor System for Smart Structure. *Key Engineering Materials*, 270-273:2114–2119.
- Kitayama, K. (1998). Code Division Multiplexing Lightwave Networks Based upon Optical Code Conversion. *IEEE Journal on Selected Areas in Communications*, 16(7):1309–1319.
- Lee, J. S. and Miller, L. E. (1998). *CDMA Systems Engineering Handbook*. Artech House.
- Nawrot, U., Geernaert, T., Pauw, B. D., Anastasopoulos, D., Reynders, E., Roeck, G. D., and Berghmans, F. (2017). Mechanical strain-amplifying transducer for fiber Bragg grating sensors with applications in structural health monitoring. In Chung, Y., Jin, W., Lee, B., Canning, J., Nakamura, K., and Yuan, L., editors, *25th International Conference on Optical Fiber Sensors*. SPIE.
- O'Farrell, T. and Lochmann, S. (1994). Performance analysis of an optical correlator receiver for SIK DS-CDMA communication systems. *Electronics Letters*, 30(1):63–65.
- Rajan, G., editor (2015). *Optical Fiber Sensors: Advanced Techniques and Applications*. CRC PR INC.
- Wang, Y., Gong, J., Dong, B., Wang, D. Y., Shillig, T. J., and Wang, A. (2012). A Large Serial Time-Division Multiplexed Fiber Bragg Grating Sensor Network. *Journal of Lightwave Technology*, 30(17):2751–2756.
- Yamaguchi, T., Arai, M., and Shinoda, Y. (2015). Development of wavelength measurement system of multiplex Fiber Bragg Gratings using Optical Frequency Domain Reflectometry. In *2015 9th International Conference on Sensing Technology (ICST)*. IEEE.